A Thermally Stimulated Current/Relaxation Map Analysis of the Relaxation Processes in Aromatic Polyester, Liquid Crystal Polymer Film

GEORGE COLLINS* and BARBARA LONG

Hoechst Celanese Research Division, Summit, New Jersey 07040

SYNOPSIS

Thermally stimulated current (TSC) and relaxation map analysis (RMA) have been applied to the examination of dynamics of thermally induced relaxation processes in highly oriented, wholly aromatic, polyester liquid crystalline polymer films. Films of two compositions were examined. A primary distinction in composition was the difference in level of 6-hydroxy-2-napthoic acid. Following an analysis protocol developed by Sauer et al., it was found that values of activation enthalpy were well above the zero entropy value at temperatures well below the Sauer "T_g." This indicates a high level of cooperativity in rotational relaxation processes even at low temperatures. Cooperative rotational relaxation domains were postulated to account for this behavior. The persistence of cooperativity above the Sauer "T_g" is evidence that these materials did not undergo a conventional glass transition at any temperature in the range −80 to 200°C. The behavior of these materials as a model system of "loosely bundled rods" was examined using a modified Barker–Crine analysis. This type of model behavior seemed to fall off at relatively low temperatures. The occurrence of rotational processes at high temperatures with little or no loss in orientation suggests that polymer chains are physically constrained to maintain their relative positions. © 1994 John Wiley & Sons, Inc.

INTRODUCTION

Thermally stimulated current (TSC) and the related relaxation map analysis (RMA) are based on the thermally activated decay of a polymer "electret." This term was introduced in 1896 to describe a dielectric material that preserves a polarization after the external field responsible for that initial polarization has been removed. In polymeric materials, such electrets can be formed when the heated dielectric polymer is cooled in the presence of a static electric field; these have been termed "thermoelectrets."[1] It has only been since 1939 that the temperature-dependent release of charge in polarized materials has been attributed to molecular motion. The development of an adequate theory of this behavior that includes polymers allows this thermally activated discharge to be used as a probe in the analysis of energetics of dipole relaxations.[2] Wholly aromatic polyester materials are good candidates for this type of analysis, because these polymers contain a potentially polarizable carbonyl dipole for each structural unit in the chain.

In conventional thermally stimulated current experiments on polymeric materials, a high-voltage, stabilized DC power supply is used to polarize a film or sheet sample between two electrodes at a temperature near or above the glass transition temperature. While being held at this temperature, a voltage on the order of 10^5–10^6 V/m is applied. The sample is held at the temperature for a specified time, after which the temperature is lowered to well below the T_g, usually to about −150°C. At this low temperature, the nonequilibrium orientation of the dipoles is fixed when the field is removed. A sensitive electrometer is used to monitor short-circuit current while the sample is heated at a constant rate. Current is generated at temperatures where sufficient

* To whom correspondence should be addressed.

Journal of Applied Polymer Science, Vol. 53, 587–608 (1994)
 CCC 0021-8995/94/050587-22

mobility is induced in the dipole sites that they can change their nonequilibrium, polarized orientation to an unoriented state that is closer to thermal equilibrium. Once relaxed, the unoriented dipoles no longer contribute to the depolarization current.

A relaxation map is the plot of the log of the relaxation time vs. the inverse of temperature. Ideally, RMA would involve the evaluation of the temperature dependence of each isolated dipole relaxation process. Because the dipole relaxations in polymers can be characterized by a distribution of relaxation times, the global TSC depolarization current represents the current produced by all these undifferentiated processes. The isolation of a narrow band of relaxations out of the full distribution can be accomplished using the "windowing polarization" technique developed in France in the early 1970s.[3-5]

In the windowing polarization method, the sample is brought to a polarization temperature (T_p) and the polarization voltage is applied. It is held at this temperature for a period of time (t_p), which allows the orientation of all the dipoles that have mobility at or below this temperature. The temperature is then lowered 2–5°C below the polarization temperature. The sample is then held at this temperature (T_d) with the voltage off for a period of time (t_d), which allows those dipoles that are mobile at or below T_d to depolarize. This leaves only those dipoles oriented that had mobility in the temperature window between T_p and T_d. At the end of the depolarization period, the temperature is lowered to T_0, where no dipole mobility is possible. From this temperature, the sample is heated with a linear program. The depolarization current that is observed results only from those dipoles that have remained oriented in the temperature window. The result of doing this at several polarization temperatures is a set of individual depolarization curves for each polarization temperature are constituitive components of a global TSC depolarization current.

A TSC without windowing polarization produces results that are similar to differential scanning calorimetry (DSC) or dynamic mechanical analysis (DMA) operating at a very low frequency (10^{-3}–10^{-4} Hz). RMA using multiple polarization windows can isolate the elementary modes of relaxation and provide a detailed probe of the range of mobilities in the internal structure of a polymeric material. The advantage of RMA is the possibility of obtaining quantitative values for the activation enthalpy as a function of temperature.

In RMA experiments, the raw data consists of a trace of current as a function of temperature. Using the Bucci formalism, these data are typically transformed to give the temperature dependence of the relaxation time[6]:

$$\ln[\tau(T)] = \ln\left\{\int_{T_0}^{T} J(T)\,dT\right\} - \ln[J(T)] \quad (1)$$

where T is the temperature position on the relaxation curve; τ, the relaxation time (s^{-1}); $J(T)$, the measured current density at temperature T; and T_0, the initial temperature of the depolarization scan. If it is assumed that all the depolarization current originates from dipole relaxation, this relaxation time can be taken to be related to an energy barrier and formulated in terms of the Eyring theory of absolute rates[7]:

$$\Delta G_p^* = \Delta H_p^* - T\Delta S_p^* \quad (2)$$

where ΔG_p^*, ΔH_p^*, and ΔS_p^* are the free energy, enthalpy, and entropy of activation, respectively. The subscript, "p," indicates that these quantities are a function of the temperature of polarization and correspond to distinct processes occurring at each polarization temperature. The relaxation time can be expressed as

$$\tau_p = \tau_{op}\exp(\Delta G_p^*/kT) \quad (3)$$

By allowing

$$\ln(\tau_{op}) = -\ln(kT/h) \quad (4)$$

the activation parameters can be determined from the depolarization data by plotting $\ln[\tau_p/(h/kT)]$ vs. $1/T$. The slope yields $\Delta H^*/k$ and the intercept yields $-\Delta S^*/k$.[8] On the basis of a discrete dipolar structural unit, the activation enthalpy is related to the phenomenological activation energy by

$$E_a = \Delta H^* + kT \quad (5)$$

On a per mole basis, k, the Boltzman constant, becomes R, the gas constant.[9]

Lacabanne et al.[10] observed that the broad mechanical relaxation process observed in the vicinity of the glass transition in polyolefins can be described by a distribution of relaxation times that collectively follow what is termed a "compensation law" that is formally expressed as

$$\tau = \tau_c\exp\left\{\frac{\Delta H^*}{k}\left(\frac{1}{T} - \frac{1}{T_c}\right)\right\} \quad (6)$$

where τ_c and T_c are compensation time and compensation temperature, respectively. The implication of this is that when a set of discrete processes are isolated by thermal windowing techniques a mechanistic coupling between these processes can be revealed by examining their compensation behavior. This examination can be carried out by observing from eq. (6) that the intercept obtained when $\ln(\tau)$ is plotted vs. $1/T$ is given by $\ln[\tau_c \exp(-\Delta H^*/kT_c)]$, while the slope will be ΔH^*. As a consequence, a plot of the intercept vs. the slope for each discrete process can produce a linear relationship when compensation phenomena are operative. The compensation frequency will be the intercept of this plot and the slope will be $-1/T_c$. When the $\ln(\tau)$ vs. $1/T$ plots for each discrete process are extrapolated to the point where these lines all intersect, that is the compensation point. At the compensation temperature, all the discrete processes that constitute the broad relaxation near the glass transition have the same relaxation time.[10]

Since the intercept of the logarithmic plot from eq. (6) is related to the activation entropy and the slope is related to the activation enthalpy, the analysis of the physical significance of compensation phenomena reduces to a determination of the possible relationship between these quantities: the activation entropy and enthalpy. This relationship was first examined in terms of the volumes of activation for diffusion in organic solid and later used to describe diffusion in amorphous polymers. Two empirical relations were established:

$$\Delta V^* = \frac{\beta \Delta S^*}{\alpha} \tag{7}$$

$$\Delta V^* = 4\beta \Delta H^* \tag{8}$$

where α is the isobaric coefficient of volume expansion, and β, the isothermal compressibility.[11,12] These equations imply that for relaxation processes the entropy and enthalpy of activation are related through the volume of activation. Typically, ΔV^* is not easily determined, but by substituting for $\Delta V^*/\beta$ from eq. (7) into eq. (8), this relationship can be expressed as

$$\Delta S^* = 4\alpha \Delta H^* \tag{9}$$

For several polymers, this relationship was shown to hold in the vicinity of their principal mechanical relaxation processes.[13] Since these parameters can be evaluated from dielectric relaxation data, this mode of analysis can applied to dipole relaxation processes.

The determination of the activation parameters from the dipole relaxation behavior permits an evaluation of the energetic constraints to the motions involved in these relaxation processes. The analysis of these constraints assists in the formulation of rational models that describe the state of aggregation of the polymer chains in the solid state. These models, in turn, can be useful in the development of structure–property relationships.

EXPERIMENTAL

The term "LCP variant" will be used to refer to two liquid crystal polymer materials that have been examined in both the untreated and heat treated forms; these variants are Vectra A and RD404. Vectra A is also known as Vectra, A950, CO, and CO 73/27. RD404 is also known as COTBP and Vectra E. These are wholly aromatic polyesters. Vectra A containins *p*-hydroxybenzoic acid (HBA) and 6-hydroxy-2-napthoic acid (HNA). RD404 contains *p*-hydroxybenzoic acid (HBA), 6-hydroxy-2-napthoic acid (HNA), terephthalic acid (TA), and 4,4′-biphenol (BP). The molar ratios for each monomer in Vectra A and RD404 has been published in the open literature.[14] The ratio of phenylene to naphylene structural units is 73/27 for Vectra A, whereas it is 96/4 in RD404.

The LCP material is used in either the extruded film or extruded tape form. In both cases, the thickness is on the order of 25–32 microns. In this report, the terms "film" and "tape" are used interchangeably. The designation "AS" is used to indicate untreated film or tape in its as-extruded form. The designation "HT" is used in indicate the film or tape in its heat-treated form. For Vectra A, the heat treatment is 1 h at 230°C followed by 16 h at 270°C. For RD404, the heat treatment is 8 h at 300°C. The Hermans orientation function for these films and tapes is on the order of 0.96, which compares with 0.96–0.98 for fibers. On the basis of this, these films are reasonable to use as models for fibers.

Each LCP film sample is carefully cut with a knife or a scalpel to avoid splintering the material. The sample's surface is free of voids, smooth, and clean to ensure a good electrode-to-sample interface. The sample surface dimensions are approximately 12 × 5 mm. The sample is loaded into sample holder contained in the TSC cell of a Solomat TSC/RMA Model 91000 instrument. The holder is the electrode assembly with a fixed bottom electrode and a pivot-disk top electrode. This holder retains the sample and provides both polarizing voltage and the mea-

suring current path. Since the samples are analyzed for transitions from high to subambient temperatures, the connection between the sample and electrodes is critical. The sample is inserted onto the bottom flat disc, avoiding sample contact with the outer electrodes to avoid, in turn, providing a conductive path between the center and outer electrodes that will short-circuit the system. Then, the top flat disc is adjusted firmly onto the sample. A heater cage is lowered over the sample holder, the cooling jacket is raised, and the cell is closed.

Moisture in the cell is removed by first purging with helium three times with alternate evacuations to 10^{-4} mbar at the vacuum manifold. To obtain this vacuum requires both a roughing (rotary vane) pump plus a diffusion pump. High-purity helium is used as the gas surrounding the sample during measurement. After the final flushing out of the system, the cooling jacket around the sample is filled with coolant (liquid nitrogen) and the TSC cell then automatically cools to +5.0°C before starting an experiment.

The TSC cell assembly is made up of the sample environment and the electronic modules for the measurement of the depolarization current. The assembly consists of the bottom cell, the top cell, and the top cell box that contains the electrometer. The bottom cell contains the cooling jacket. The top cell contains the sample holder, the protective Faraday cage, the heating coil, the temperature measuring sensor, and the polarization/depolarization electrodes. The solenoid device selects either polarization voltage or depolarization current at the sample electrodes. When polarization voltage is applied at a selected temperature, mobile dipoles in the sample will align in the electric field defined by the voltage drop across the electrodes. The raw data produced during depolarization is a profile of current vs. temperature that represents the current generated by the motion of the aligned dipoles as they relax to a nominally unaligned thermal equilibrium. The principal independent experimental variable is the polarization temperature (T_p). Typically, the temperature at the maximum in depolarization current (T_m) is 8–10°C higher than the T_p. Both T_p and T_m are well within the range where the depolarization current is recorded. In this report, T_p is indicated as the independent variable for the extraction of activation parameters.

The RMA batch protocol is a series of windowed experiments. By varying the value of the temperature of polarization and running multiple experiments, the elementary modes can be isolated or windowed and used to construct a relaxation map. A single sample is analyzed by multiple experiments of varying polarization temperatures ranging from 200.0 to −80.0°C at 5.0°C increments. The sample is first polarized at temperature T_p for 2.0 min to allow orientation of a certain fragment of dipoles, then quenched as fast as possible to 2.0°C below the T_p. The field is removed and this temperature is held for 2.0 min. This allows depolarization of low activation energy dipoles. Finally, at a rate of 30.0°C/min, the sample is cooled to 70.0°C below the T_p, held for 1.0 min, then heated to 200.0°C at 7.0°C/min. The resulting depolarization current is measured and corresponds only to the relaxation of those dipoles with activation energies isolated in that 2°C temperature window. The RMA data for LCP film samples is a series of depolarization current profiles obtained at the different polarization temperatures. The Solomat instrument control software allows each batch experiment to be run in an unattended mode.

A simple TSC procedure is run on all the samples prior to the RMA batch experiment in order to give them the same thermal history. For this procedure, the sample is first polarized by applying a dc voltage of 50.0 V/mm for 5.0 min at 25.0°C. The material is then quenched as fast as possible to −100.0°C and allowed to stabilize for 5.0 min to freeze the internal structure. The field is then removed. The sample is heated at a constant rate of 7.0°C/min to 250.0°C and the resulting depolarization current is measured by the TSC electrometer. No attempt is made to analyze the depolarization current observed from this procedure; it is carried out only to provide a nominally uniform thermal history for each specimen.

TSC batch experiments were conducted on LCP film samples at two temperatures: first, polarization at "T_g" (the Sauer glass transition discussed later), and, second, polarization at Ipk max (the RMA depolarization current maximum). Both "T_g" and Ipk max were determined by RMA batch experimental data. For both TSC batch experimental methods, the sample is polarized using 2000.0 V/mm for 5.0 min, then quenched to −150.0°C under field and then depolarized at 7.0°C/min to 200.0°C. The TSC batch procedure involves carrying out this sequence three times for each specimen.

RESULTS AND DISCUSSION

The extruded tape is oriented and taken to be a two-dimensional model for the highly oriented fiber. In the tape form, the molecules are oriented in the di-

rection of extrusion. It is known from high-temperature wide-angle X-ray experiments that there is nearly no loss in orientation when fibers are heated.[15] Under this constraint, the molecular structure requires that the observed dipole relaxations occur by rotational motions nominally about the axis of the oriented macromolecule. Support for this assertion is provided by the high dependence of absorption of radio-frequency (rf) power on orientation of fibers in the field. For the case where the applied rf field is perpendicular to the fiber axis, the absorption is sufficient to melt the filaments in a few seconds, whereas when the applied rf field is parallel to the fiber axis, the absence of temperature increase indicates little rf absorption.[16] The restriction of induced motion to rotational processes greatly simplifies the image of the physical processes responsible for the relaxation current produced in RMA and TSC experiments.

Relaxation Map Analysis (RMA)

The thermal windowing technique provides a means to determine the activation enthalpy and activation entropy at various temperatures of polarization. Sauer et al. developed an interpretive scheme that allows information about the relaxation processes to be extracted from the dependence of activation enthalpy and activation entropy on polarization temperature. Based on the molecular-kinetic model developed by Adam and Gibbs, changes in the activation parameters are taken as manifestations of changes in the cooperative nature of motions in the assembly of polymer chains.[17-19] Sauer et al. gave the relationship between activation energy and temperature as

$$E_a = \Delta H^* + RT$$
$$= RT[24.76 + \ln(T/f)] + T\Delta S^* \quad (10)$$

This equation describes the physical relationship between cooperative and uncooperative motions. For the situation where relaxation motions are localized and uncooperative, the activation energy should represent the energy barrier for the local motion of an isolated structural unit in the polymer molecule. For this isolated motion, there is only a small, near zero, contribution to the configurational entropy of the polymer chain, so that ΔS^* is nominally zero and the activation energy has a nearly linear dependence on temperature. The idealized behavior for polymers is that below the glass transition (T_g) motions are localized to individual structural units, and above T_g, in the equilibrium melt, the free volume is sufficiently large that segmental motions are relatively uncorrelated. In these two temperature regions, ΔS^* in eq. (10) approaches zero. In the vicinity on the low-temperature side of T_g, however, the situation is more complicated. In this temperature range, the motions typically are more complex than are isolated structural units and motions become cooperative because the free volume is not large enough to accommodate the motions that are possible at that temperature. The interchain interaction influences the physical chain trajectory and gives rise to an increase in the magnitude in the change in configurational entropy. By eq. (13), this increase in entropy change should produce an increase in activation energy. Sauer et al. illustrated this behavior for poly(ether ketone ketone) (PEKK) in Figure 7 of Ref. 15. By this mode of analysis, T_g is given by the nearly singular maximum of the E_a vs. T_p plot.

Figure 1 shows the activation enthalpy [Fig. 1(A)] and the activation entropy [Fig. 1(B)] as a

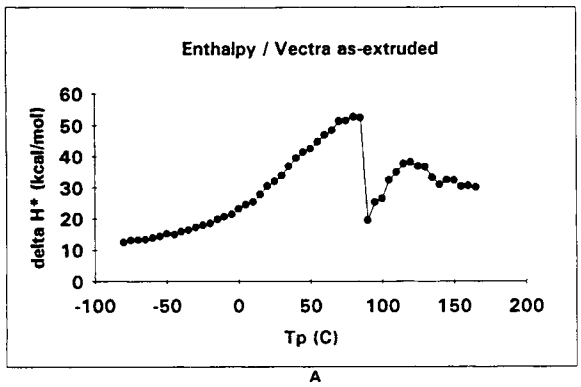

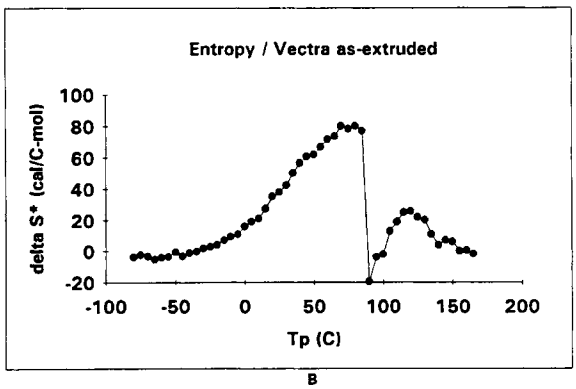

Figure 1 (A) Relaxation enthalpy (ΔH^*) vs. polarization temperature (T_p) for as-extruded Vectra. (B) Relaxation entropy (ΔS^*) vs. polarization temperature (T_p) for as-extruded Vectra.

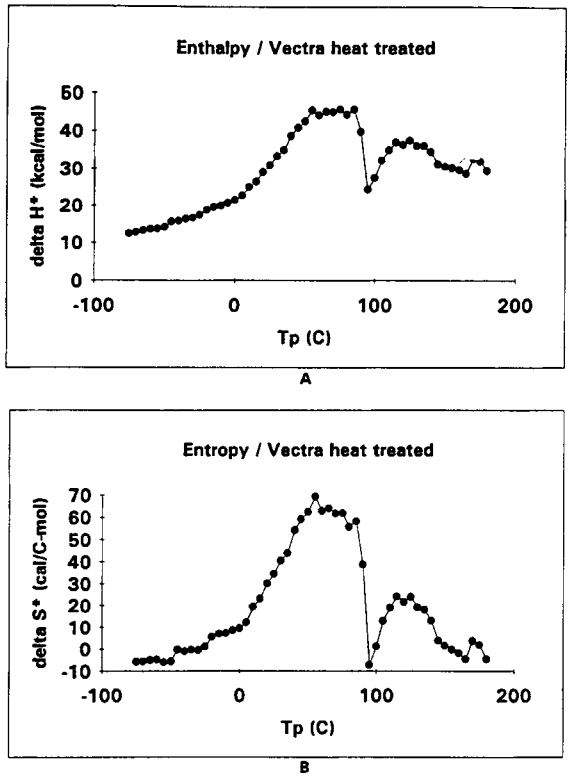

Figure 2 (A) Relaxation enthalpy (ΔH^*) vs. polarization temperature (T_p) for heat-treated Vectra. (B) Relaxation entropy (ΔS^*) vs. polarization temperature (T_p) for heat-treated Vectra.

function of polarization temperature for as-extruded Vectra tape. Figure 2 shows the same data obtained for the heat-treated Vectra tape. In general, while the sharp singular behavior is not evident, there is a qualitative similarity between these data and that given by Sauer et al. There is a discontinuity in the temperature dependence of activation enthalpy for both as-extruded and heat-treated tape. Figure 3 plots the activation enthalpy data for both as-extruded and heat-treated Vectra tapes on the same scale, which reveals a striking similarity to their behavior below, at, and above the discontinuity. The "zero entropy" line in Figure 3 is the temperature dependence of activation enthalpy calculated using eq. (10) with activation entropy set to zero. In this equation, f is the effective frequency of the temperature scan that was estimated as 3×10^{-4} s^{-1}. The energy barriers to conformational changes that do not produce loss in orientation of the ester linkage (R and T rotors) are estimated to be a maximum of 5 kcal/mol in aromatic esters.[20] Even at low temperatures, the values for activation enthalpy are well above that value. As the T_p approaches the discontinuity from the low-temperature side, substantial values of activation enthalpy develop, reaching values as high as 50 kcal/mol in the vicinity on the low-temperature side of the discontinuity. These relatively high values indicate that the motions associated with the rotational dipole relaxation processes are cooperative over this temperature range.

According to the Sauer et al. analysis, this discontinuity would represent the glass transition in as much as it is a manifestation of the increase in free volume to the point that uncooperative rotations can take place. The decoupling of cooperative motions at the discontinuity results in a drop in the

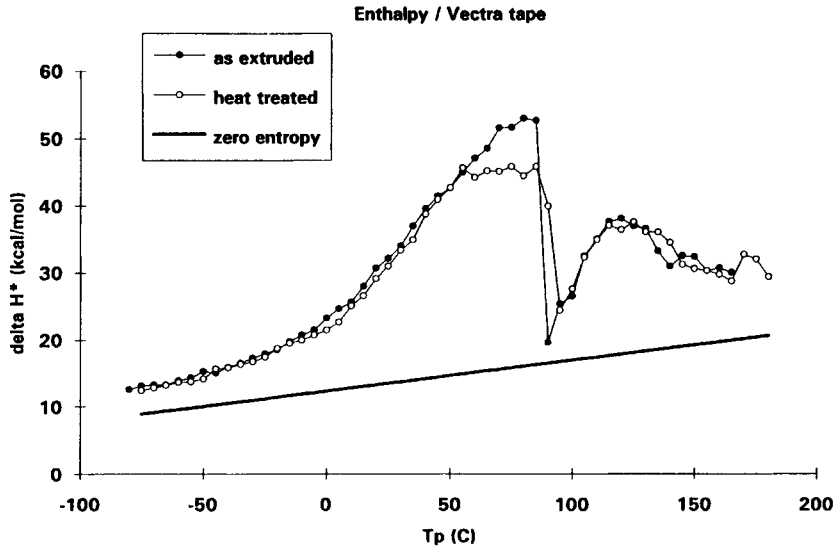

Figure 3 Comparison of experimental relaxation enthalpy with calculation from eq. (10) assuming zero entropy: (●) as-extruded Vectra; (○) heat-treated Vectra; (——) calculated.

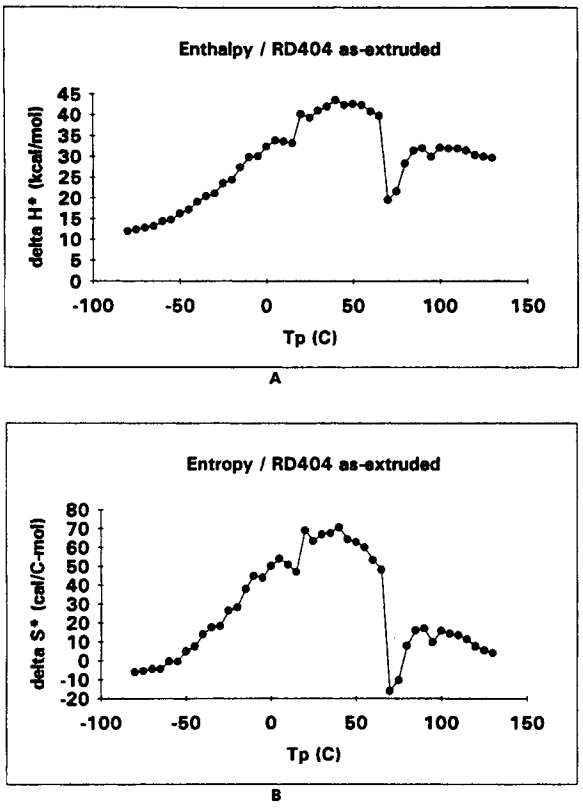

Figure 4 (A) Relaxation enthalpy (ΔH^*) vs. polarization temperature (T_p) for as-extruded RD404. (B) Relaxation entropy (ΔS^*) vs. polarization temperature (T_p) for as-extruded RD404.

activation enthalpy and entropy. Ideally, above the glass transition, the relaxation behavior should be similar to that in a liquid in that rotational motions should be uncorrelated. However, the data in Figures 1 and 2 clearly show an increase in activation enthalpy and entropy at temperatures above the discontinuity. This is indicative of the redevelopment of cooperative processes and implies that the observed discontinuity does not represent a T_g in the idealized sense. Instead, this must be taken as a modified relaxation process that will be designated as the Sauer "T_g."

Figure 4 shows the activation enthalpy [Fig. 4(A)] and activation entropy [Fig. 4(B)] as a function of polarization temperature for as-extruded RD404 tape. Figure 5 shows the same parameters obtained for heat-treated RD404. Figure 6 plots the activation enthalpy data for both as-extruded and heat-treated RD404 on the same scale.

The features of the profiles of activation enthalpy for RD404 are qualitatively similar to that of the Vectra tape. In all cases, there is an increase in both the activation enthalpy and entropy as the temperature is increased from −80°C. There is a discontinuous change in these parameters that corresponds to the Sauer "T_g" followed by an increase in the value of these parameters after the "T_g." Adopting the convention that "T_g" is taken as the last point before a large decrease in activation enthalpy, the positions of "T_g" are tabulated Table I.

The values for the activation enthalpy for the Vectra tape are marginally, but consistently, higher than those values for RD404. The enthalpy values at the "T_g" are 45–50 kcal/mol for the Vectra tape, whereas they are about 40 kcal/mol for RD404.

From dynamic mechanical and dielectric relaxation spectroscopy experiments, it has been reported that the relaxation processes occurring in the low-temperature region involve what have been described as "local" rotations of phenyl and napthyl structural units.[21–24] For a strictly localized process, the activation enthalpy is not expected to show a strong dependence on temperature. The fact that this increasing activation enthalpy with polarization temperature is observed in the relaxation behavior

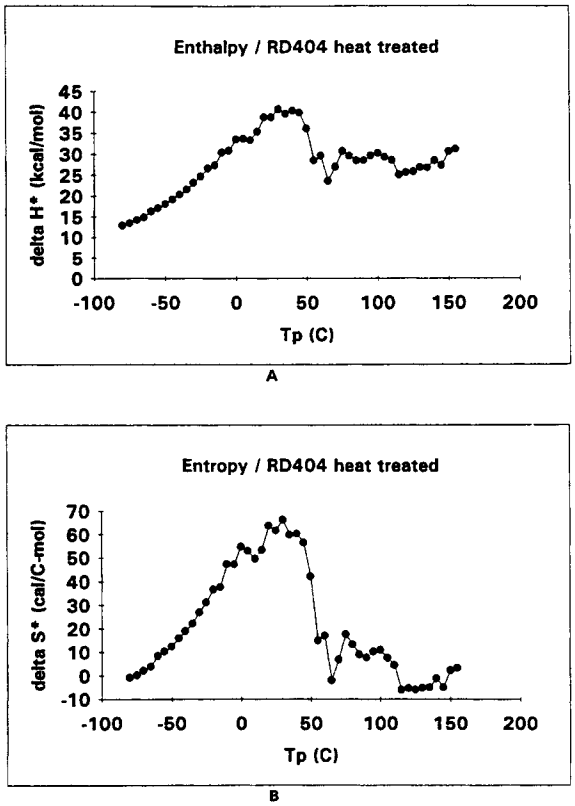

Figure 5 (A) Relaxation enthalpy (ΔH^*) vs. polarization temperature (T_p) for heat-treated RD404. (B) Relaxation entropy (ΔS^*) vs. polarization temperature (T_p) for heat-treated RD404.

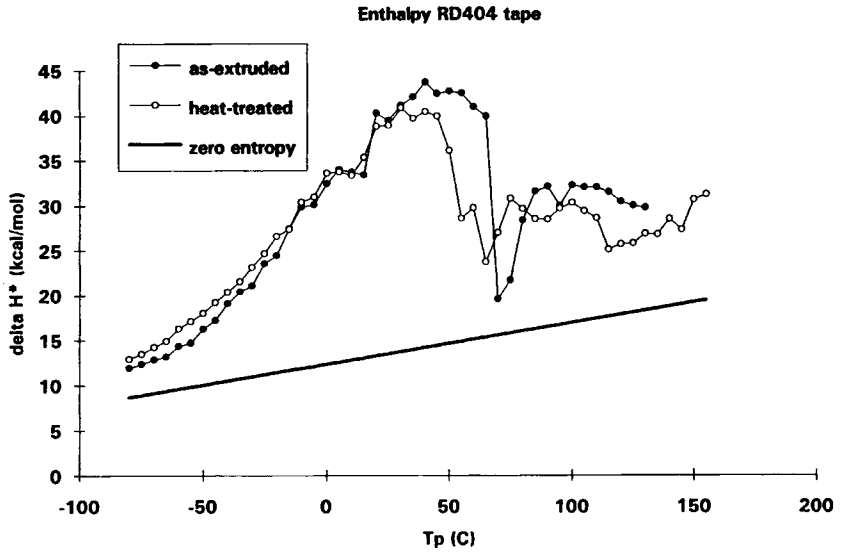

Figure 6 Comparison of experimental relaxation enthalpy with calculation from eq. (10) assuming zero entropy; (●) as-extruded RD404; (○) heat-treated RD404; (——) calculated.

for every oriented LCP tape sample strongly indicates that in the temperature range of investigation strictly localized rotational relaxations are not operative even at temperatures well below the Sauer "T_g."

A perspective on this behavior can be formulated by considering cooperativity in conformational relaxations arising from the close proximity of structural units on neighboring chains. Matsuoka and Quan as well as Adachi developed models in which the entity undergoing rotational relaxation is not an isolated structural unit but a cooperative domain in which all individual structural units undergo rotational relaxation synchronously.[25,26] By these models, the domain is characterized by the number of conformers in the domain.

By identifying the conformer with the structural unit, the observed activation energy will be the product of the activation energy for the isolated structural unit multiplied by the number of structural units in the cooperative domain. The cooperativity arises as a consequence of the close proximity of segments that causes structural units to be meshed so that they can only relax together in an intermeshed rotational mode. This situation is depicted Figure 1 from Ref. 25.

Table I Sauer "T_g" (°C)

	As-extruded	Heat-treated
Vectra	85	85
RD404	65	45

The behavior of the LCP tapes suggests that the polymer chains are in close proximity to each other. The increase in temperature provides the necessary kinetic energy for the onset of rotational motion in the structural units. That motion, however, is obstructed by the structural units on the neighboring chain. In order for the rotational relaxation to take place, the target structural unit and its neighbor(s) must cooperatively rotate. Clearly, the activation energy for this process is higher than that of the isolated unit, because it must account for the barriers to rotation of all the units that are collectively undergoing this rotational motion. It appears that for the oriented tape samples the LCP molecules in each variant in both as-extruded and heat-treated states are in sufficiently close proximity to impose cooperative rotational relaxation processes from the low end of the experimental temperature range to the "T_g."

As previously mentioned, the fact that the activation enthalpy falls abruptly at "T_g" but increases at higher temperatures indicates that this is not a conventional glass transition. Indeed, the temperature, 85°C, observed for the "T_g" of the Vectra tapes is substantially lower than the 110–125°C reported for the α-transition in previous publications.[21–24] Since the conventional glass transition is associated with the onset of larger-scale segmental motion, it is necessary to compare this "T_g" with some measure of motion. The raw data produced in

these RMA experiments is a profile of relaxation current vs. polarization temperature. The current is taken to originate in the motion of the carbonyl dipole, so that the relaxation current is a direct indicator of the occurrence of dipolar motion. The formal relationship between current and the number of relaxing dipoles to produce the current is given by the Frohlich equation[27]:

$$\frac{1}{\varepsilon_0 E_p A}\int_{T_0}^{\infty} J(T)\,dT = \frac{3\varepsilon_s}{(2\varepsilon_s + \varepsilon_{\inf})}\frac{4\pi N}{3kT}\left(\frac{\varepsilon_{\inf}+2}{3}\right)^2 g\mu_0^2 \quad (11)$$

where ε_0 is the permittivity of free space; E_p, the polarization field; A, the area of the sample between the electrodes; ε_s, the static permittivity with dipoles oriented in field but immobile; $\varepsilon_{\inf}$, the permittivity at high temperature where orientation does not

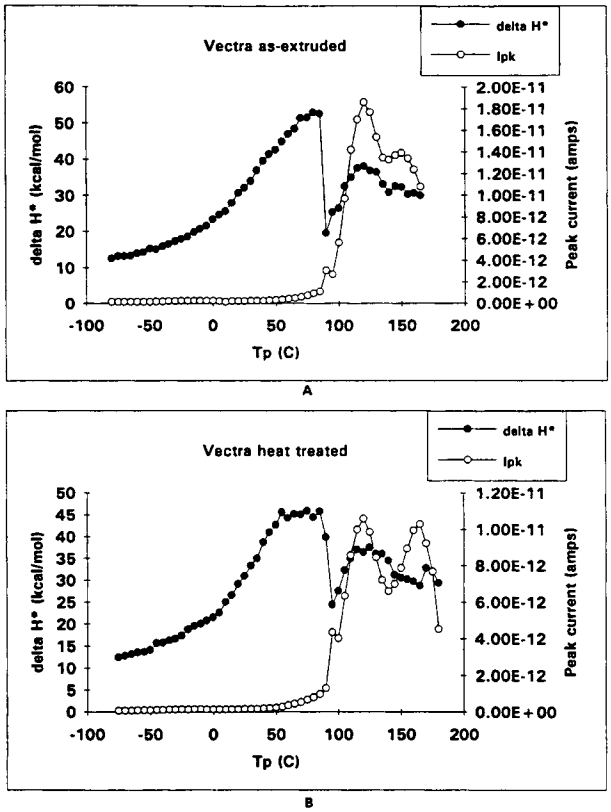

Figure 7 (A) Relaxation enthalpy (ΔH^*) and peak relaxation current (Ipk) vs. polarization temperature (T_p) for as-extruded Vectra: (●) ΔH^*; (○) Ipk. (B) Relaxation enthalpy (ΔH^*) and peak relaxation current (Ipk) vs. polarization temperature (T_p) for heat-treated Vectra: (●) ΔH^*; (○) Ipk.

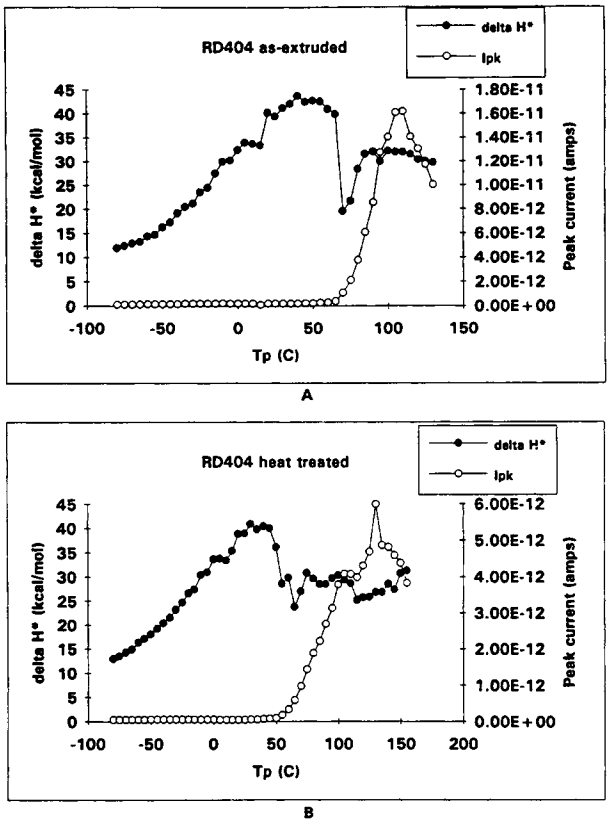

Figure 8 (A) Relaxation enthalpy (ΔS^*) and peak relaxation current (Ipk) vs. polarization temperature (T_p) for as-extruded RD404: (●) ΔH^*; (○) Ipk. (B) Relaxation enthalpy (ΔH^*) and peak relaxation current (Ipk) vs. polarization temperature (T_p) for heat-treated RD404: (●) ΔH^*; (○) Ipk.

contribute; N, the number of dipoles per unit volume, and μ_0, the external moment of the isolated dipole. The factor g is an orientation correlation function that is often taken as unity. The temperature T in this equation would be taken as the polarization temperature, T_p. In the case of the LCP tapes, there are very large differences between the magnitudes of the peak currents for windowed polarizations below "T_g" and windowed polarizations above "T_g" that make it possible to determine the temperature regions where relaxation motion increases by a simple inspection of the peak current profile.

Figures 7 and 8 compare on overlaid plots the profiles of activation enthalpy and the maximum depolarization current for each LCP variant, both as-extruded and heat-treated. In all cases, the maximum in depolarization current occurs at polarization temperatures above "T_g" as determined by the discontinuous drop in ΔH^*. The positions of the

Table II Sauer "T_g" and Depolarization Current Maxima Temperatures (°C)

	Vectra AS	Vectra HT	RD404 AS	RD404 HT
"T_g" (°C)	85	85	65	45
Max 1 (°C)	120	120	110	105
Max 2 (°C)	150	165	NA	(135)

"T_g" along with the positions of the maxima in current are tabulated in Table II. From Figures 7 and 8, the "T_g" seems to have a specific relationship to the depolarization current; the drop in activation enthalpy, in every case, corresponds to the onset of the increase in depolarization current. At temperatures below "T_g," the peak current is on the order of 10^{-13} amps, while above "T_g," the peak current is on the order of 10^{-11} amps, an increase of two orders of magnitude. It is unambiguous that the number of dipoles undergoing relaxational motion is higher above the Sauer "T_g" than at the Sauer "T_g." It is clear from this that the Sauer "T_g" cannot correspond to a conventional glass transition process as long as the convention of rotational mobility is adopted. It is also clear, however, that this "T_g" represents a reproducible thermally induced event in the solid state of these LCP materials.

The drop in activation enthalpy followed by an increase in the magnitude of this parameter suggests that there is a restructuring of cooperative rotational relaxation domains at the Sauer "T_g." The minima in activation enthalpy in the vicinity of "T_g" ranges from 16.4 to 24.4 kcal/mol and approaches the zero entropy line. Above the "T_g," the enthalpy increases to values ranging from 30.3 to 38.1 kcal/mol. If it is assumed that the conformer elements operative above the "T_g" are the same elements that are responsible for the maximum in enthalpy at the "T_g," then it would follow that the nature of this restructuring is a reduction in the size of the cooperative domain. Using the previously cited value of 5 kcal/mol for the energy barrier for rotation of an isolated structural unit taken to represent the conformer, Vectra would have 9–10 conformer elements per domain at "T_g" and 7–8 above "T_g." RD404 would have about 8 conformers per domain at "T_g" and 6–7 per domain above "T_g." It is important to note that even at the highest temperatures examined in these studies the activation enthalpy remains at about 30 kcal/mol for all the sample tapes. The implication of this result is that there is no thermally induced loss of cooperativity. The relaxation behavior suggests that the polymer chains are held in close proximity to each other over the entire experimental temperature range. This, in turn, would suggest that at no point does this system of oriented wholly aromatic polyester chains undergo a process that can be likened to a conventional glass transition. At no point does it undergo a transition that results in a loss of cooperative relaxations.

From Figures 7 and 8 and the Table II, it is apparent that the peak relaxation current has two maxima in the case Vectra and two maxima in every heat-treated case. In the previous paragraph, the increase in relaxation current after "T_g" was associated with the restructuring of cooperative rotational relaxation domains. Consistent with that interpretation is the possibility that the second maximum is a consequence of a further restructuring of these domains as induced by the further increased temperature.

Compensation Behavior

The discussion of eq. (6) in the Introduction section indicated that a set of mechanistically correlated processes can be observed as a distribution of relaxation times that collectively follow a compensation law. The windowing polarization technique is particularly well suited for examining this behavior because of its ability to isolate nominally discreet processes within a distribution of processes. This is accomplished by plotting the intercept vs. the slope from the Arrhenius plot of each polarization window or by plotting the entropy of activation vs. the enthalpy of activation of each polarization window. In both cases, the occurrence of a linear relationship over a range of data indicates compensation behavior for that subset of isolated processes represented by those windows of polarization. Once that subset has been identified, eq. (6) predicts that there is a temperature, T_c, at which all the correlated relaxation processes in this subset will have the same relaxation time (inverse of compensation frequency). This means that if the Arrhenius data from each polarization window experiment are all plotted in the same data space, then they will extrapolate to a common point called the "compensation point."

Figure 9 illustrates the compensation behavior for the high-temperature polarizations, whereas Figure 10 illustrates the compensation behavior for the low-temperature polarizations. Clearly, for the high-temperature data, the extrapolation is to low temperature and higher frequency, whereas for the low-temperature data, the extrapolation is to higher temperature and low frequency. This change in di-

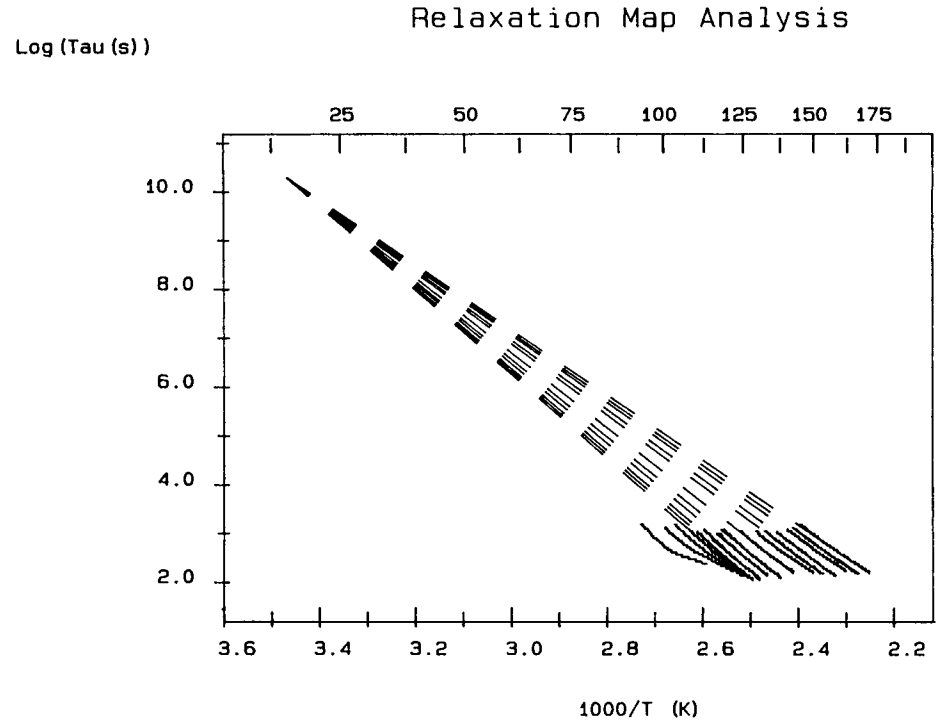

Comp= (Tc = 15.30 C, log(tau) = 10.27)

Figure 9 Extrapolated relaxation map at higher polarization temperatures.

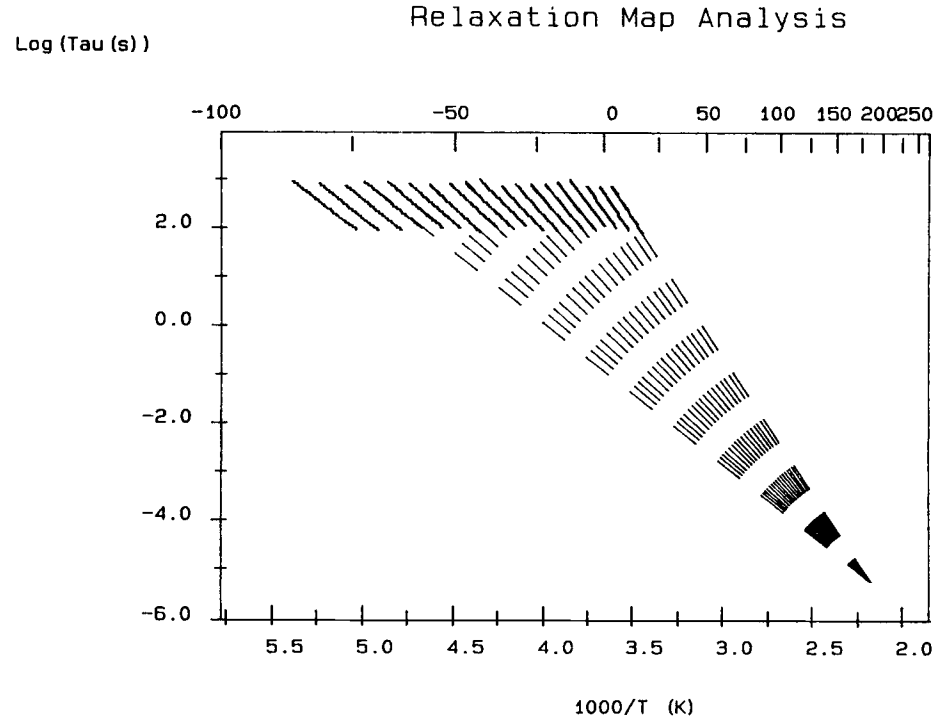

Comp= (Tc =185.45 C, log(tau) = -5.20)

Figure 10 Extrapolated relaxation map at lower polarization temperatures.

rection of extrapolation has been described as the "Z-structure" by Ibar and is claimed to be a general feature of polymer behavior across the T_g.[8] In our experiments, the change in directionality across the Sauer "T_g" has been taken as an indication of a restructuring of the mode of cooperativity in the rotational relaxations as the temperature is raised or lowered across the "T_g." It is important to observe in Figure 10 that at the lowest polarization temperatures (−80 to −70°C) compensation behavior does not appear to be operative, as indicated by the inability to extrapolate these relaxation map lines. This suggests the onset of isolated, uncorrelated rotational motion at these lowest temperatures.

The qualitative features of the extrapolated relaxation map plots for all the extruded film variants in both the as-extruded and heat-treated forms were similar to that shown for the as-extruded Vectra film, indicating that in all cases there is a restructuring of the mode of cooperativity across the Sauer "T_g."

Ratio of Activation Entropy to Activation Enthalpy

The Lawson–Keyes relationship between entropy of activation and enthalpy of activation was briefly described in the Introduction and quantified as eq. (9). This equation is an empirical relationship that arises from the examination of diffusion of small molecules in solids. The point of relevancy is that diffusion of small molecules in polymer solids is accomplished by the free volume created by changes in the conformations between structural units of the polymer chain. For the extruded LCP films used in these experiments, conformational changes are observed as depolarization current, making it possible to use the entropy and enthalpy of activation derived from these RMA experiments to probe the ratio $\Delta S^*/\Delta H^*$ using the Lawson–Keyes equation. Table III gives the temperature position of the Sauer "T_g" along with the ratio of the entropy to the enthalpy of activation at that "T_g." The last column gives the coefficient of volume expansion obtained using eq. (9). The values for the $\Delta S^*/\Delta H^*$ ratios for all the variants are in the range of 0.00121 to 0.00146/°C. When compared to the values compiled by Eby, these values are most like the values at the glass transitions in polytetrafluoroethylene with $\Delta S^*/\Delta H^* = 0.0018/°C$ and polychlorotrifluoroethylene with $\Delta S^*/\Delta H^* = 0.0016/°C$. The value for the only polyester listed by Eby, poly(ethylene terphthalate), is $\Delta S^*/\Delta H^* = 0.002/°C$.[13]

Table III Lawson–Keyes Parameters

Variant	"T_g" (°C)	$\Delta S^*/\Delta H^*$ ($°C^{-1}$)	$(\Delta S^*/\Delta H^*)/4$ ($°C^{-1}$)
Vectra AS	85	0.00146	0.000366
Vectra HT	85	0.00127	0.000319
RD404 AS	65	0.00121	0.000303
RD404 HT	45	0.00142	0.000354

As an approach to understanding how the anharmonicity of the between-chain binding forces influence the thermal expansivity, Barker developed an expression for the Gruneisen constant in terms of the entropy and volume of activation. The Gruneisen constant relates the change in lattice frequency with change in volume. Since the between-chain forces are much weaker than the intrachain bonds, it is more likely that the between-chain vibrations will become anharmonic at a given temperature. As a consequence, the between-chain modes make a larger contribution to the Gruneisen constant than do the intrachain modes. This is formally known as Wada's hypothesis and has the consequence that polymer systems can be modeled as a loosely bundled system of rods.[28] Crine further developed the Barker model by observing that the constant 4 in the Lawson–Keyes equation [eq. (9)] was actually a parameter related to interchain vibrations through the Gruneisen constant. He approximated the Lawson–Keyes ratio as[29–31]

$$\Delta S^*/\Delta H^* = \frac{2}{3} + \frac{2}{T} + \frac{2\alpha^2}{3} T \qquad (12)$$

This equation allows the formalism developed for the model of a loosely bundled system of rods to be compared with experimentally obtained values for the $\Delta S^*/\Delta H^*$ ratio over the full temperature range of the experiment.

Figures 11 and 12 show the $\Delta S^*/\Delta H^*$ plots for each variant as extracted from polarization window experiments. All variants, both as-extruded and heat-treated, show similar behavior in that for each case the data go through a maximum in the temperature region just below the "T_g." The Sauer "T_g" is visible as a sharp minimum in the data. Interestingly, the value of the maximum is about 0.0015/°C in all the cases shown. Since the entropy of activation is functionally related to the enthalpy of activation through the activation volume, the similar values is suggestive of similar activation volumes in the vicinity of the "T_g." This point was not examined in any further detail. The shape of the experimental data immediately reveals that eq. (12) cannot de-

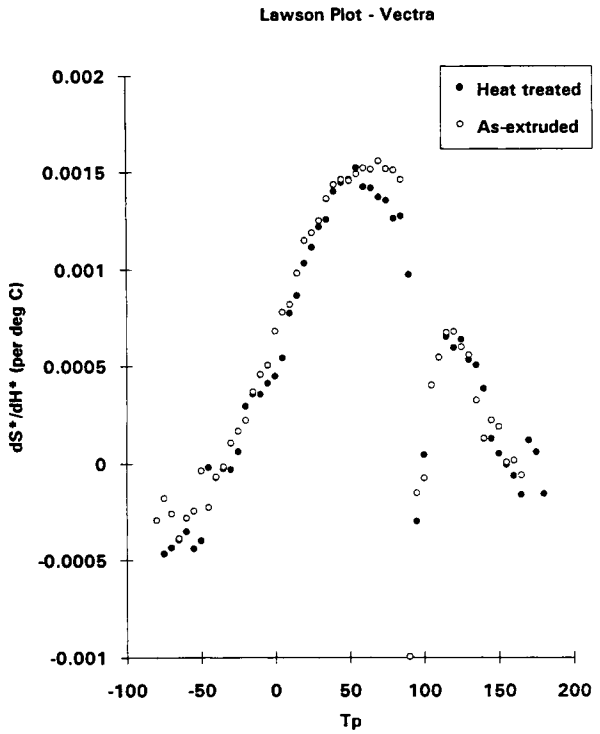

Figure 11 Lawson plot, $\Delta S^*/\Delta H^*$ vs. T_p, for Vectra: (○) as-extruded; (●) heat-treated.

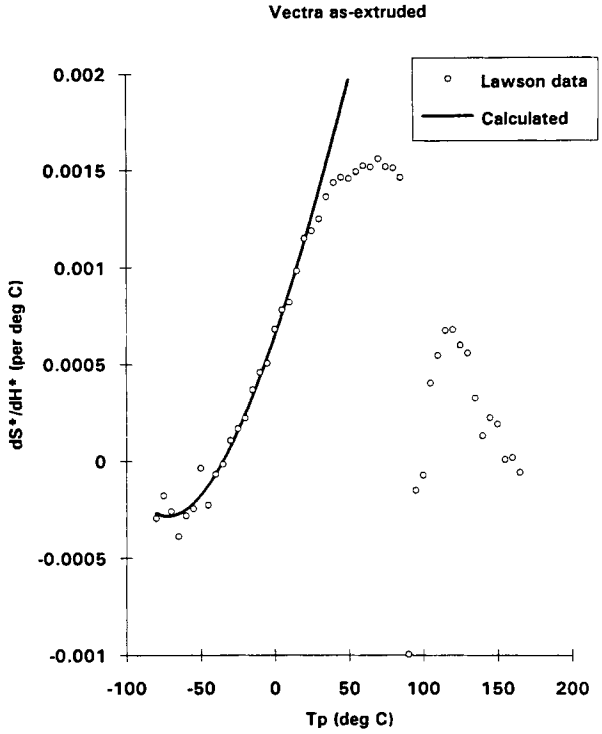

Figure 13 Comparison of Lawson ratio with calculation using eq. (13) for Vectra as-extruded: (○) Lawson ratio; (——) calculated.

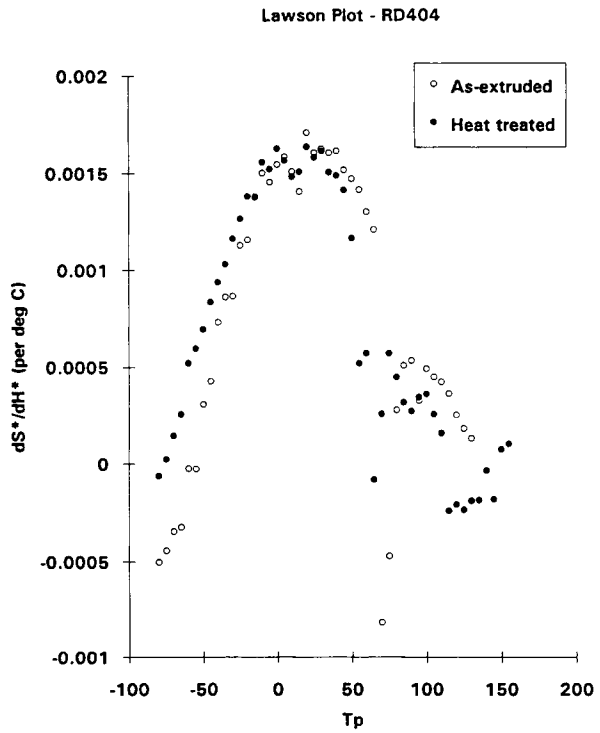

Figure 12 Lawson plot, $\Delta S^*/\Delta H^*$ vs. T_p, for RD404: (○) as-extruded; (●) heat-treated.

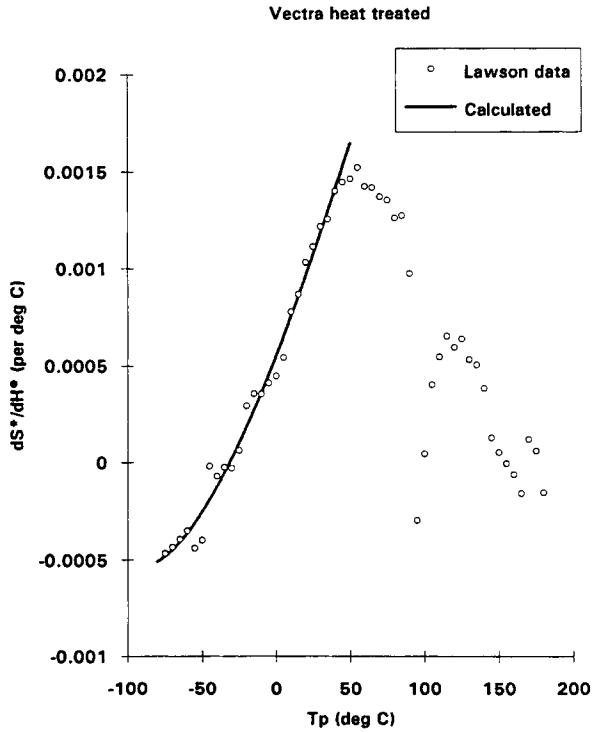

Figure 14 Comparison of Lawson ratio with calculation using eq. (13) for Vectra heat-treated: (○) Lawson ratio; (——) calculated.

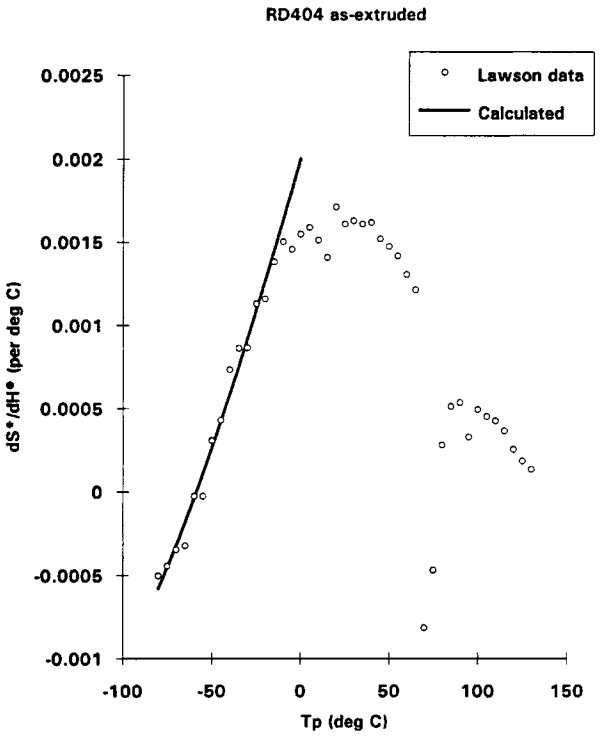

Figure 15 Comparison of Lawson ratio with calculation using eq. (13) for RD404 as-extruded: (○) Lawson ratio; (——) calculated.

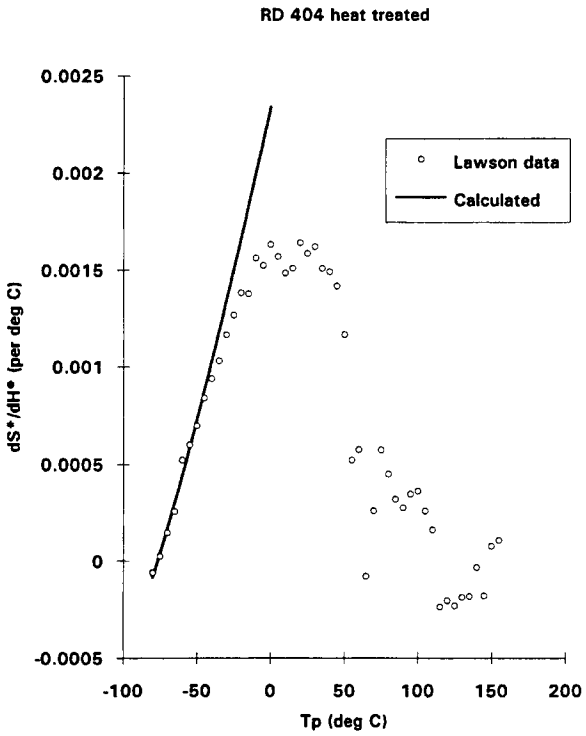

Figure 16 Comparison of Lawson ratio with calculation using eq. (13) for ED404 heat-treated: (○) Lawson ratio; (——) calculated.

scribe the behavior over the full temperature range. The form of this equation is such that it monotonically increases at high temperature and no maximum is possible. Because an increase in $\Delta S^*/\Delta H^*$ with temperature is only observed on the low-temperature side of the maximum, only this region of the data was considered to be described by this equation. A generalized form of eq. (12) was used and fit to the data:

$$\Delta S^*/\Delta H^* = a + \frac{b}{T} + cT \qquad (13)$$

Figures 13–16 show how this equation was fit to as-extruded and heat-treated data for each variant. In Table IV, the fitting parameters are indicated for each sample; the last column is a calculated coefficient of volume expansion in this temperature region using the assumption that $c = 3\alpha^2/2$ from eqs. (12) and (13).

There is one interesting feature about the parameters: The "a" parameter is consistently negative for these materials rather than the $\frac{2}{3}$ predicted by eq. (12). It is difficult at this point to assign any specific physical meaning to these parameters, but this phenomenon will be examined further in future experiments. If this equation can be taken as a representation of the polymer molecule system behaving as an assembly of loosely bundled rods, then, clearly, that description degrades on the low-temperature side of the "T_g" and is no longer represen-

Table IV Fitting Parameters for Crine Equation

Variant	a	b	c	α
Vectra AS	−0.0199015	1.97116	0.0000488219	0.00856
Vectra HT	−0.0130771	1.13214	0.0000347371	0.00722
RD404 AS	−0.0154648	0.978237	0.0000508619	0.00873
RD404 HT	−0.0126077	0.753993	0.0000446428	0.00818

tative. The failure of the equation to describe the data at increasing temperatures has to be rooted in the failure of the potential function developed by Barker to describe the between-chain interaction. It suggests that at these increased temperatures the rotational behavior of the structural units in the chain are such that they preclude the loosely bundled rod model description.

Global Thermally Stimulated Current (TSC)

In addition to windowing polarization experiments, global polarization experiments were conducted to examine these LCP film samples in a mode that would be similar to manner in which DSC experiments are conducted. To do this, samples are polarized at both the Sauer "T_g" and at the temperature at which the maximum in depolarization current that was observed in the windowed polarization experiments. Consistent with what was observed in the RMA experiments, the magnitude of the TSC depolarization current was much lower for polarizations at the Sauer "T_g" than for polarizations at the RMA current maxima (see Figs. 7 and 8). Because of this difference, only data from TSC polarizations at the RMA current maxima will be presented. For the Vectra tape, the TSC polarization temperature was 120°C, and for RD404, the polarization temperature was 110°C. Figures 17–20 show the experimentally obtained depolarization current over the full temperature range for each variant in both as-extruded and heat-treated forms. Figures 21–24 show the current peaks that occur in the low-temperature range on an expanded scale. On each graph there are three current traces, because each experiment was conducted by performing three polarization–depolarization operations. In all cases, the first depolarization trace differs distinctively from the subsequent two traces. In Figures 17–24, two depolarization traces will nearly overlap each other, while one will clearly diverge in magnitude from the two that overlap. The divergent trace is always the first trace.

No previous information on Vectra-like materials in static field dielectric experiments, TSC, is available; however, it is possible to compare the peak positions observed in our experiments with those observed in oscillating field experiments by calculating the shift in the position of the relaxation peak on the basis the activation energy for the relaxation process using the following equation:

$$T_2 = \left[\frac{E_a T_1}{E_a - RT_1 \log f_2 + RT_1 \log f_1}\right] - 273 \quad (14)$$

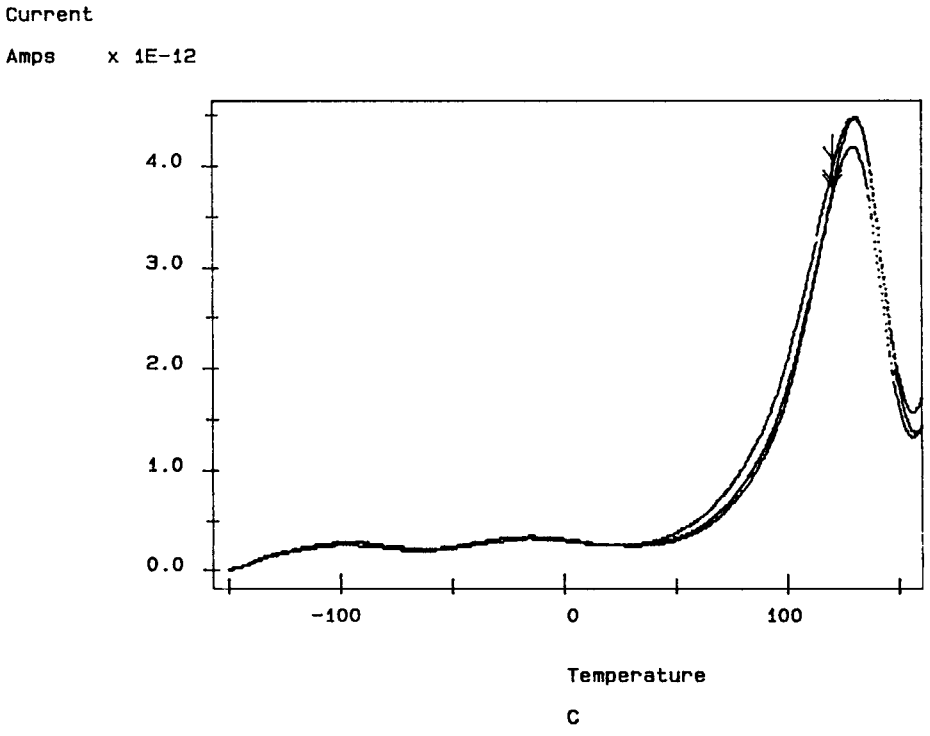

Figure 17 TSC depolarization current profiles, T_p = 120°C, for Vectra as-extruded.

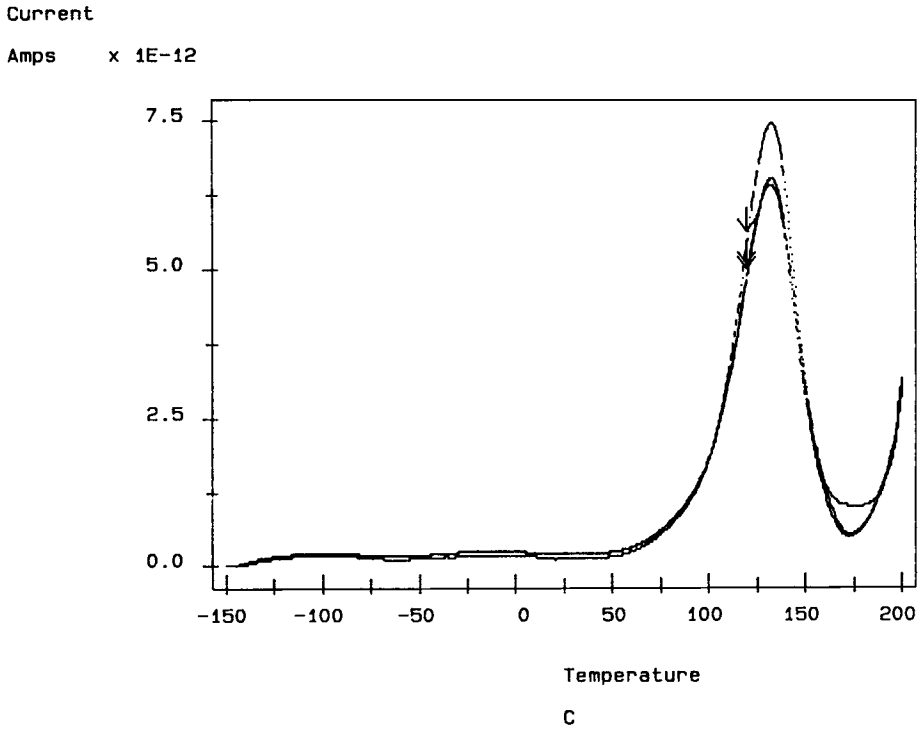

Figure 18 TSC depolarization current profiles, T_p = 120°C, for Vectra heat-treated.

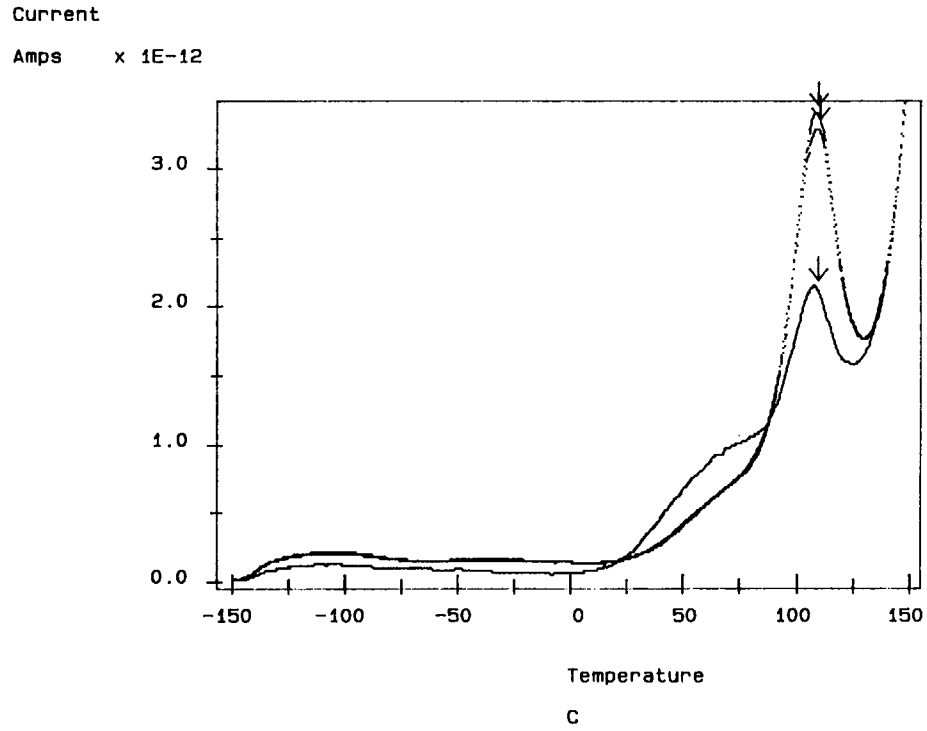

Figure 19 TSC depolarization current profiles, T_p = 110°C, for RD404 as-extruded.

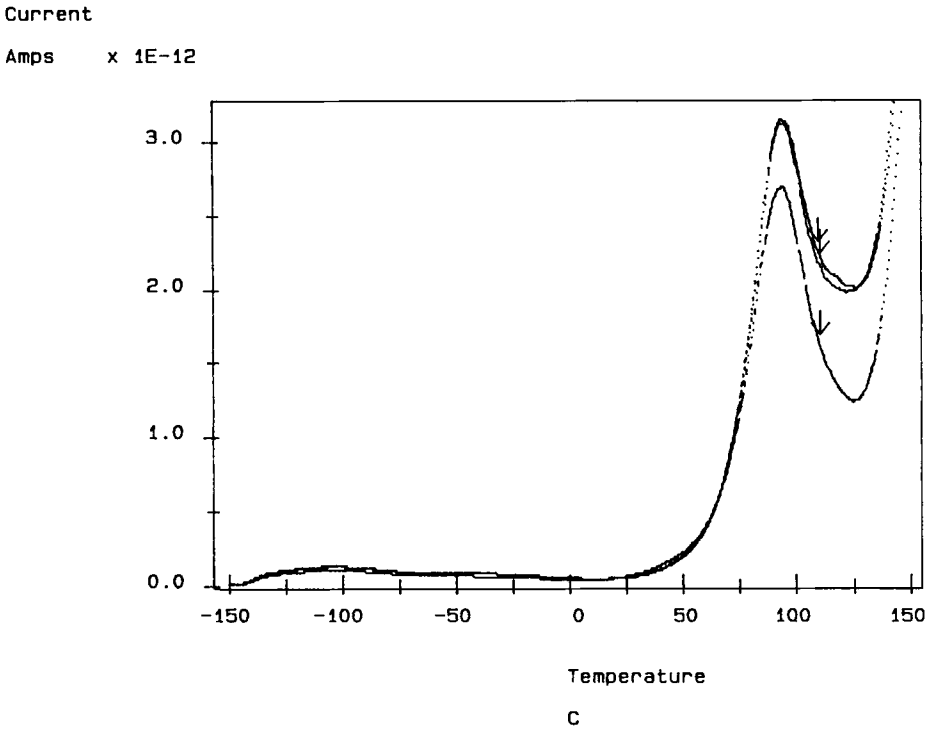

Figure 20 TSC depolarization current profiles, T_p = 110°C, for RD404 heat-treated.

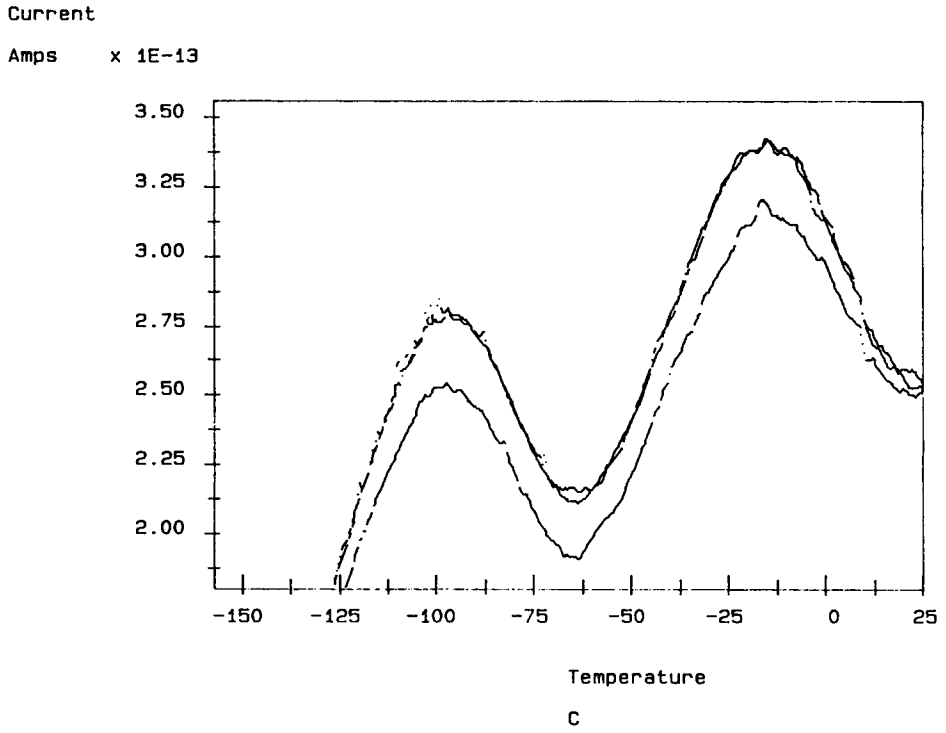

Figure 21 TSC depolarization current profiles, T_p = 120°C, for Vectra as-extruded; low-temperature scale expansion.

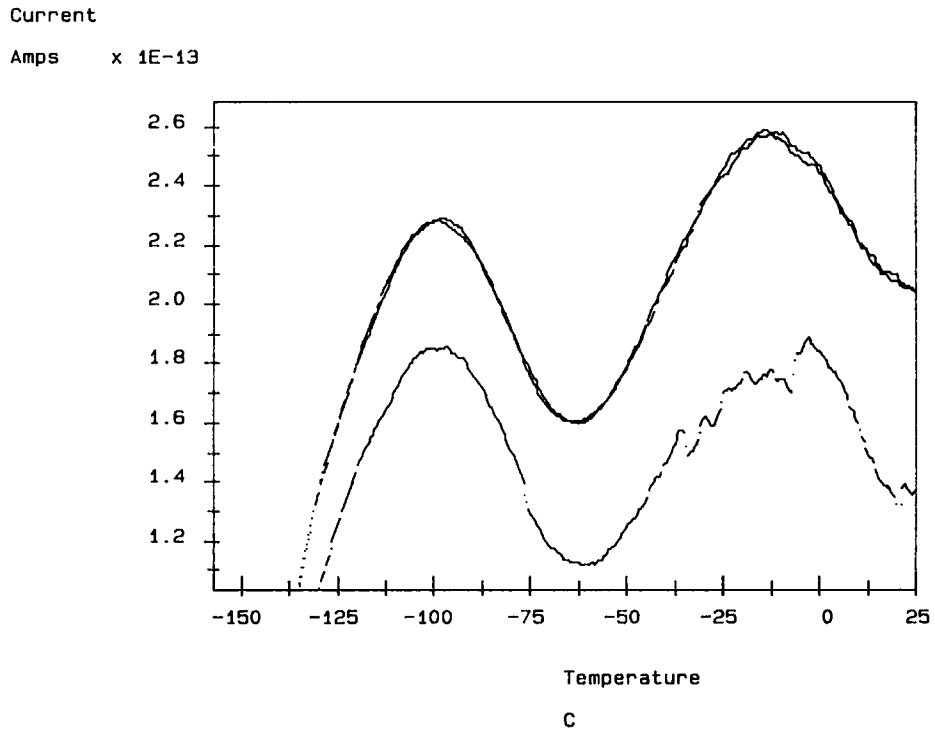

Figure 22 TSC depolarization current profiles, T_p = 120°C, for Vectra heat-treated; low-temperature scale expansion.

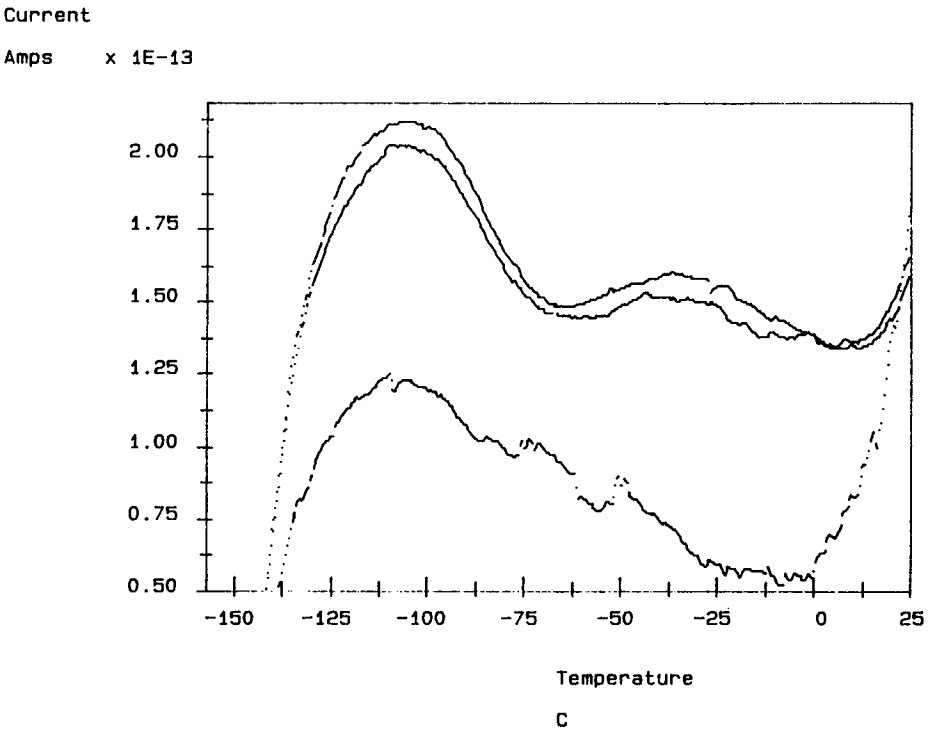

Figure 23 TSC depolarization current profiles, T_p = 110°C, for RD404 as-extruded; low-temperature scale expansion.

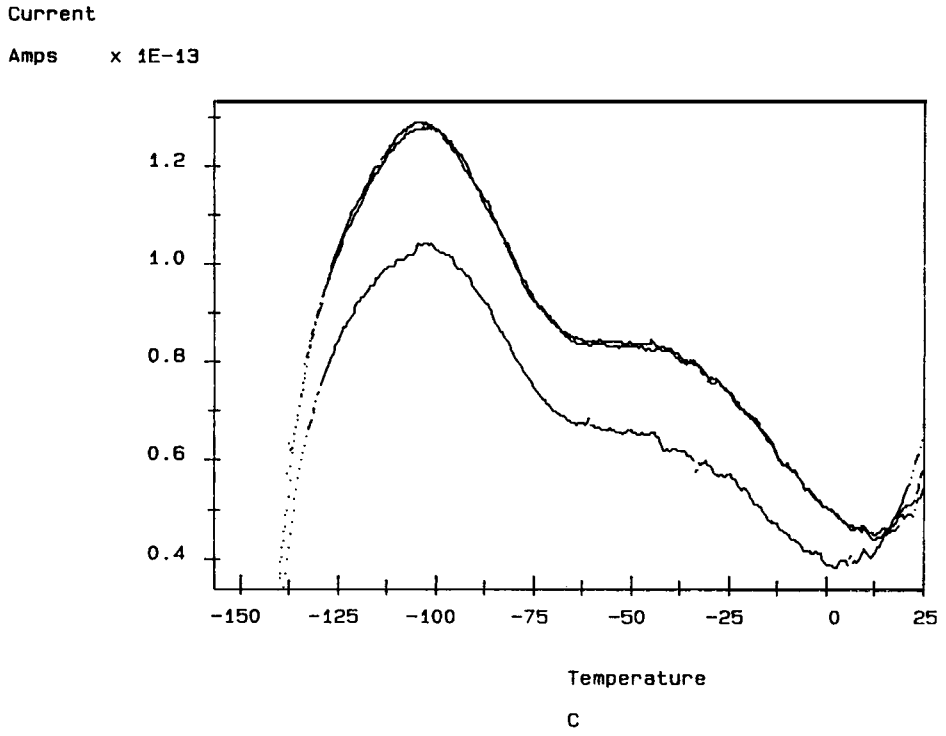

Figure 24 TSC depolarization current profiles, T_p = 110°C, for RD404 heat-treated; low-temperature scale expansion.

where E_a is the activation energy obtained from Arrhenius analysis in oscillating field experiments, and T_1, the position of the relaxation process at frequency f_1. T_2 is the temperature to which the relaxation process is shifted when observed at frequency f_2. Activation energies for the alpha (170 kcal/mol), beta (25 kcal/mol), and gamma (12 kcal/mol) processes observed in Vectra materials have been reported from the laboratory of Ward in the frequency range of 1–10 kHz.[23] The effective frequency in the TSC experiments is on the order of 3×10^{-4}, so that the calculated positions of these processes at this frequency are compared with the observed TSC peaks in Table V.

Table V Calculated and Observed Transition Temperatures (°C)

Variant	Gamma	Beta	Alpha
Calculated	**−105**	**−26**	**97**
Vectra AS	−97	−15	129
Vectra HT	−98	−13	132
RD404 AS	−106	−35	109
RD404 HT	−104	−40	94

The calculated positions should apply most closely to the "Vectra AS" variant, since the activation energies were determined with this material. There is relatively large difference between the calculated position of the alpha process at the TSC effective frequency and that observed in the TSC experiment, but because of the steepness of the line in the Arrhenius plot for this process, the value of the activation energy determined from that slope has some uncertainty associated with it. On the basis of this calculation, the two peaks observed at low temperature are nominally associated with the phenyl unit rotations (−106 to −97°C) and the naphthyl unit rotations (−41 to −13°C) as has been previously described.[21,22]

Comparing the as-extruded and heat-treated forms of each variant, there seems to be little change in positions of any of the processes when Vectra tape is heat-treated, whereas for the RD404, there is a discernible shift of the alpha process to lower temperature with heat treatment. There is a distinct difference in the position of the beta process for RD404 compared to Vectra. If the beta process arose from the rotational relaxations of isolated naphthyl units, such a large difference in the position of this process would not be expected. If, instead, this pro-

cess is associated with a cooperative rotational relaxation domain that is rich in naphthyl units, this behavior becomes more intelligible. If it is accepted that the naphthyl unit has an intrinsically higher activation energy for rotation because of its structure, then the drop in the temperature of the beta process for RD404 occurs because this composition contains a lower number of naphthyl units in it, which would, in turn, mean that there are fewer naphthyl units in the cooperative domains that relax in this temperature region. Because there are fewer naphthyl units, the activation energy of the domain is raised to a lesser extent and the temperature of relaxation will be lower than in the case of Vectra. The shift in the beta process from −15°C in Vectra to −35°C in RD is consistent with this interpretation.

The relative magnitude of the depolarization current for the beta process is also suggestive of the presence of cooperative domains. For strictly isolated rotations, it would be expected that the magnitude of the depolarization current for the gamma and beta processes should be in proportion to the number of equivalents present. However, for Vectra, which is 73% HBA and 27% HNA, Figures 21 and 22 clearly indicate that the beta depolarization current associated with the HNA relaxations at −15 and −13°C is higher than the HBA depolarization current at −97 and −98°C even though the HNA content is lower than the HBA content. This is possible because the cooperative domains that contain HNA also contain a fraction of HBA. When the rotational relaxation event takes place, all the constituents of the domain move synchronously. As a result, the current that is observed is produced from both the HNA and the coupled HBA. In Vectra, the fraction of coupled HBA is large because the level of HNA is relatively high at 27%. For RD404, depolarization current for the beta process at −35 and −40°C in Figures 23 and 24 is higher than 4% of the current for the gamma process, as might be expected for strictly isolated rotations. This higher than expected current originates in the same phenomenon of coupling HBA units to HNA units in cooperative rotational relaxation domains: Only for RD404 is the HNA content low; the number of coupled HBA units is also lower.

It is of interest to examine the change in the magnitude of the depolarization current on heat treatment because any substantial reduction in the current would indicate the immobilization of the available dipoles in rigid structures. Since the films were of different thickness, this comparison was crudely made by dividing the peak current at each relaxation process by the thickness of the film. Since the sampling area of the electrode is constant in all experiments, the raw current in amps is used in this comparison. Table VI illustrates that comparison where d is the thickness of the film in meters.

Focusing on the depolarization current per unit thickness of the alpha process, this quantity marginally increases on heat treatment for Vectra while it decreases for RD404. Considering the order of magnitude change in peak depolarization current in going from the alpha process to the two low-temperature processes, the changes observed between as-extruded and heat-treated forms do not appear to be as significant. If there is immobilization, it is not manifest in this crude quantity for Vectra and it is not of a large enough extent in RD404 to produce an order of magnitude reduction in the depolarization current. This suggests that substantially most of the dipoles remain mobile after heat treatment.

CONCLUSIONS

The temperature dependence of activation enthalpy from RMA data, showing an increase as the temperature is increased from −80°C, provides a rather clear indication that a high degree of cooperativity is required for the rotational dipole relaxation processes to occur even at low temperature. An abrupt drop in the activation enthalpy at a temperature that has been designated the Sauer "T_g" is evidence that the system restructures or repartitions how that

Table VI Relative Current at Each Relaxation Process

Variant	d (m)	Gamma (amp/m)	Beta (amp/m)	Alpha (amp/m)
Vectra AS	25×10^{-6}	1.12×10^{-8}	1.36×10^{-8}	1.78×10^{-7}
Vectra HT	28×10^{-6}	8.18×10^{-9}	9.21×10^{-9}	2.32×10^{-7}
RD404 AS	24×10^{-6}	8.83×10^{-9}	6.67×10^{-9}	1.43×10^{-7}
RD404 HT	25×10^{-6}	5.16×10^{-9}	3.36×10^{-9}	1.26×10^{-7}

cooperativity is distributed internally. Above this "T_g," a higher rotational mobility is allowed, as evidenced by the increased magnitude of the depolarization current. The nature of this restructuring is difficult to specify, although it is clear that it facilitates the lowering of the activation enthalpy. Global TSC results suggest the occurrence of cooperative rotational relaxation domains. The experimentally determined activation enthalpy will correspond to the rotational energy barrier of the domain, rather than to the individual structural unit. It may be that in response to the increase in temperature the number of conformers in the domain is reduced, which lowers the activation enthalpy of the domain and allows the observed increase in current. Even after this restructuring, the activation enthalpy remains higher than the 5 kcal/mol that might be expected for isolated rotation. This seems to suggest that although the spatial extent of correlation may be reduced the rotational processes are still cooperative up to the highest temperatures in our experiments. This is taken to indicate that the polymer chains are in close proximity to each other over the full temperature range examined. It appears that at no point do these systems undergo a glass transition in the sense that allows uncorrelated rotational relaxation processes.

The distinctions in behavior between Vectra and RD404 are subtle. RD404 undergoes the Sauer "T_g" process at lower temperatures than does Vectra in as-extruded and heat-treated forms. However, the positions of the maxima in depolarization current are higher for RD404 than for Vectra in the heat-treated form. The results suggest that the large-scale rotational motion implicated by the depolarization current above the Sauer "T_g" is harder to initiate in RD404 than in Vectra, which may indicate a marginally tighter packed internal structure than in the other variants.

Peak currents from global TSC experiments and values of polarization from RMA experiments indicate that the rotational mobility of the polymer molecules is largely maintained in going from as-extruded to heat-treated forms. A mechanism for large-scale immobilization of dipoles on heat treatment does not seem to operate. The implication is that the development of tensile properties on heat treatment must arise from some process other than extensive conventional crystallization that would be accompanied by dipole immobilization.

The Barker–Crine analysis attempts to examine the region over which these systems can be considered to behave as "loosely bundled rods." This has its appeal because of the conventional concept of Vectra systems as assemblies of rigid rod molecules. To the extent that the equations we have employed represent this behavior, it seems to fall off at relatively low temperatures. Since orientation is not lost in the experimental temperature range, this would indicate that the persistent liquid crystal-like behavior of these systems does not seem to arise from the linearly extended lattice intermolecular potentials necessary to describe rods. These potentials are based on lattice vibrations that lose their applicability with the onset of rotational processes. Rather than being constrained on a lattice, it is possible that the polymer chains are physically constrained in a manner that allows rotational processes to occur, but that does not allow the chains to change their relative positions so that orientation is maintained.

We acknowledge the contribution of Mr. William Pleban of Hoechst Celanese in the setup and initial operational development of the Solomat instrument. We also acknowledge the many useful discussions with Dr. J.-P. Ibar and Mr. Rick McIntyre of Solomat.

REFERENCES

1. B. Tareev, *Physics of Dielectric Materials* (English Translation) Mir, Moscow, 1975, p. 215.
2. J. van Turnout, *Polym. J.*, **2**(2), 173 (1971).
3. D. Chatain, P. Gautier, and C. Lacabanne, *J. Polym. Sci. Phys.*, **11**, 1631 (1973).
4. J. P. Ibar, P. Denning, T. Thomas, A. Bernes, D. de Goys, J. R. Saffell, P. Jones, and C. Lacabanne, in *Polymer Characterization: Physical Property, Spectroscopic and Chromatographic Methods*, C. D. Carver and T. Provder, Eds., American Chemical Society, Washington, DC, 1990, Chap. 10.
5. A. Bernes, R. F. Boyer, D. Chatain, C. Lacabanne, and J. P. Ibar, in *Order in the Amorphous "State" of Polymers*, S. E. Keineth, R. L. Miller, and J. K. Rieke, Eds., Plenum, New York, 1987, p. 305.
6. C. Bucci and R. Fieschi, *Phys. Rev.*, **148**(2), 816 (1966).
7. S. Glasstone, K. J. Laidler, and H. Eyring, *The Theory of Rate Processes*, McGraw-Hill, New York, 1941, p. 195ff.
8. J. P. Ibar, *Polym. Eng. Sci.*, **31**(20), 1467 (1991).
9. H. W. Starkweather, *Macromolecules*, **14**, 1277 (1981).
10. C. Lacabanne, D. Chatain, J. C. Mopagens, A. Hiltner, and E. Baer, *Solid State Commun.*, **27**, 1055 (1978).
11. R. W. Keyes, *J. Chem. Phys.*, **29**(3), 467 (1958).
12. A. W. Lawson, *J. Chem. Phys.*, **32**(1), 131 (1960).
13. R. K. Eby, *J. Chem. Phys.*, **37**(12), 2785 (1962).
14. D. I. Green, G. R. Davies, I. Ward, M. H. Alhaj-Mo-

hammed, and S. Abdul Jawad, *Polym. Adv. Tech.*, **1,** 42 (1990).
15. C. Saw, Hoechst Celanese Research Division, unpublished results, Dec., 1992.
16. K. Chiang and E. Chenevey, Hoechst Celanese Research Division, unpublished results, March 1993.
17. B. B. Sauer, P. Avakian, and H. W. Starkweather, in *Proceedings 12th North American Thermal Analysis Society,* Sept. 22–25, 1991, p. 17.
18. G. Adam and J. H. Gibbs, *J. Chem. Phys.*, **43**(1), 139 (1965).
19. B. Sauer and P. Avakian, *Polymer,* **33**(24), 5128 (1992).
20. P. Coulter and A. H. Windle, *Macromolecules,* **22,** 1129 (1989).
21. H. N. Yoon and M. Jaffe, Abstract of Papers, 185th American Chemical Society National Meeting, March 20–25, Seattle, WA, 1983, Abstract ANYL-72.
22. D. J. Blundell and K. A. Buckingham, *Polymer,* **26,** 1623 (1985).
23. M. H. Alhaj-Mohammed, G. R. Davies, S. Abdul Jawad, and I. Ward, *J. Polym. Sci. Part B Phys.*, **26,** 1751 (1988).
24. M. J. Troughton, G. R. Davies, and I. M. Ward, *Polymer,* **30,** 58 (1989).
25. S. Matsuoka and X. Quan, *Macromolecules,* **24,** 2770 (1991).
26. K. Adachi, *Macromolecules,* **23,** 1816 (1990).
27. N. G. McCrum, B. E. Read, and G. Williams, *Anelastic and Dielectric Effects in Polymer Solids,* republished by Dover, Mineola, NY, 1991, p. 89.
28. R. E. Barker, *J. Appl. Phys.*, **38**(11), 4234 (1967).
29. J.-P. Crine, *J. Macromol. Sci.-Phys.*, **B23**(2), 201 (1984).
30. J.-P. Crine, *IEEE Trans. Elect. Insul.*, **EI-22**(2), 169 (1987).
31. J.-P. Crine, *J. Appl. Phys.*, **66**(3), 1308 (1989).

Received August 11, 1993
Accepted January 31, 1994